Depletion Interactions in the Protein Limit: Effects of Polymer Density Fluctuations

Amit M. Kulkarni,[1] Avik P. Chatterjee,[2,*] Kenneth S. Schweizer,[1,2] and Charles F. Zukoski[1]
[1]*Department of Chemical Engineering, University of Illinois, Urbana, Illinois 61801*
[2]*Departments of Materials Science & Engineering and Chemistry, University of Illinois, Urbana, Illinois 61801*
(Received 8 March 1999)

We report the first observations of nonmonotonic changes in the second virial coefficients of protein solutions, B_2, as the concentration of nonadsorbing polymer is increased. The observed minimum in B_2 cannot be predicted from standard depletion interaction energy models and is closely associated with proximity to the lower critical solution temperature of the polymer solution. The location, depth, and molecular weight dependence of the minima are captured by the thermal polymer reference interaction site model for depletion interactions, where the polymer mesh size is a function of temperature.

PACS numbers: 61.25.Hq, 64.75.+g, 82.70.Dd, 87.15.Kg

The addition of nonadsorbing macromolecules to a stable particle suspension results in a polymer-mediated "depletion attraction" between particle pairs. Qualitatively, this induced interaction arises from an unbalanced osmotic pressure due to the excluded volume driven expulsion of polymers from the region between the particles. This phenomenon has significant scientific and technological consequences in diverse fields and has seen extensive investigation [1]. Most studies consider the "colloid limit" where the particle radius R greatly exceeds a statistically averaged measure of polymer size, the radius of gyration R_g. The model proposed by Asakura and Oosawa (AO) was the first to describe the depletion effect in the colloid limit [2]. This approach approximates a flexible polymer chain as a rigid sphere of radius R_g, ignores polymer-polymer interactions (dilute macromolecule, or "ideal solution" limit), and treats particle-particle and particle-polymer interactions as hard core repulsions. The AO model has been employed to interpret direct measurements of depletion forces [3–5], and as an effective pair decomposable potential, $U(r)$, in a one-component description of the properties of nondilute colloidal suspensions [1]. Specifically, the AO depletion potential is [2]

$$U(r) = -\frac{4}{3}\,\pi d^3 n_p kT\left[1 - \frac{3r}{4d} + \frac{r^3}{16d^3}\right], \qquad 2R \le r \le 2d \tag{1}$$

and zero (∞) for $r > 2d$ ($r < 2R$), where $d = R + R_g$, and n_p is the polymer number density. The AO potential has a spatial range of $2R_g$ and a strength determined by the ideal gas law for the polymer osmotic pressure. Although useful for many situations, the AO model has obvious limitations, e.g., it cannot address semidilute solutions, where the macromolecule concentration exceeds the threshold c_p^* for polymer-polymer interpenetration or variable polymer-solvent interactions ("solvent quality"). Verma and coworkers [5] have recently examined dilute suspensions of colloidal particles dissolved in DNA ($R \cong 2.5R_g$) solutions in a nearly "athermal" regime. Although fairly successful in dilute DNA solutions, under semidilute conditions both the amplitude and spatial range of the depletion potential were qualitatively changed due to the reduction of the polymer mesh size or density-density correlation length, ξ_ρ [3].

A much less well-studied regime is motivated by the use of nonadsorbing uncharged polymers to aid protein separations or crystallization [6]. Here $R_g/R \ge 1$, resulting in "long range" attractive depletion forces between globular proteins. For protein crystallization, a commonly used nonionic, water soluble polymer is poly(ethylene glycol) (PEG) with the chemical formula—$(CH_2\text{-}CH_2\text{-}O)_{N^-}$. PEG has the useful advantage of interacting weakly with protein molecules [6]. PEG/water solutions phase separate upon heating, giving rise to a lower critical solution temperature (LCST). As the phase boundary is approached, the mesh size grows significantly thus altering the depletion potential between proteins which can be thermodynamically quantified through the second virial coefficient, B_2. In this Letter we present the first systematic measurements of B_2 in aqueous protein-PEG solutions as a function of three dimensionless variables: size ratio R_g/R, polymer concentration c_p/c_p^*, and reduced temperature T/T_c, where T_c is the critical temperature for polymer-solvent phase separation.

The globular protein studied is hen egg white lysozyme ($R \cong 1.7$ nm) purchased from Seikagaku America Inc., which is used without further purification. The protein was dissolved in salt-water-PEG solutions (sodium acetate buffer at pH 4.6 with ionic strength controlled by the addition of NaCl). All experiments were performed at 25 °C unless stated otherwise. The lysozyme second virial coefficient is directly related to the protein-protein potential of mean force $V(r)$ as

$$B_2 = 2\pi \int_0^\infty r^2 (1 - e^{-V(r)/kT})\, dr\,. \tag{2}$$

Details of sample preparation and static light scattering methods of measuring B_2 are provided elsewhere [7]. PEG of molecular weights $M_w = 1000$, 6000, and 12 000 were purchased from the Sigma Chemical Company. For quantitative characterization purposes, the osmotic pressure of each PEG solution was measured in the absence of protein but under identical solvent conditions, for polymer concentrations up to slightly above the semidilute threshold

 0031-9007/99/83(22)/4554(4)$15.00

$(c_p/c_p^* \leq 2)$. This data [8] can be employed to estimate M_w, the polymer statistical segment length, σ, and dilute-semidilute crossover polymer concentration, c_p^*.

To interpret the osmotic pressure data, we have employed the analytic version of the microscopic polymer reference interaction site model (PRISM) integral equation theory [9], which has been shown to agree well with experiments on dilute and semidilute athermal polymer solutions [10] and also with scaling approaches [11]. The theoretical expression for the polymer osmotic pressure is

$$\frac{\Pi(z)\sigma^3}{kT} = \frac{z}{N} + \frac{\pi}{36}\left(\sqrt{\frac{12}{N}}\right)z^2 + \frac{\pi^2 z^3}{324}, \qquad (3)$$

where $\sigma = \sigma_0$ for $c_p < c_p^*$ and $\sigma_0\ (c_p/c_p^*)^{-1/8}$ in the semidilute regime [11], and $z = \rho_p\sigma^3$ is the reduced polymer segment number density. The theory also predicts the athermal mesh length is $\xi_\rho^{-1} = \sqrt{12/N}\,\sigma^{-1} + (\pi z/3\sigma)$, and based on the monomer mass, the segmental degree of polymerization is $N = M_w/44$. Fitting the osmotic pressure data with Eq. (3) over the entire polymer concentration range studied for all samples yields $\sigma_0 = 0.80 \pm 0.05$ nm. We then estimate the dilute solution $R_g = \sqrt{N/6}\,\sigma_0 = 1.43$, 3.54, and 5.38 nm for PEG 1000, 6000, and 12 000 samples, respectively [8], in good agreement with prior studies [12]. Thus, the protein-polymer size ratios are roughly $R/R_g = 1.19$, 0.48, and 0.32. Directly from the osmotic pressure data, we obtain estimates of the semidilute crossover concentration of $c_p^* \cong 0.125$, 0.025, and 0.018 g cm^{-3} for PEG 1000, 6000, and 12 000, respectively, in agreement with prior work [12].

The influence on depletion interactions of forces governing protein interactions in the absence of polymer has been characterized by measuring B_2 as a function of ionic strength. Assuming lysozyme can be modeled as a dielectric hard sphere of radius 1.7 nm [7], the protein charge q and Hamaker coefficient A were extracted by fitting the B_2 data to the standard potential model [13] consisting of the sum of electrostatic repulsion (V_R) and van der Waals attraction (V_A).

$$V_R(r) = 4\pi\varepsilon\left[\frac{qe}{4\pi\varepsilon R(1+\kappa R)}\right]^2\left(\frac{R^2}{r}\right)\exp[-\kappa(r-2R)], \qquad (4a)$$

$$V_A(r) = \begin{cases} \infty, & r < 2R + \delta, \\ -\frac{A}{6}\left[\left(\frac{2R^2}{r^2-4R^2}\right) + \left(\frac{2R^2}{r^2}\right) + \ln\left(\frac{r^2-4R^2}{r^2}\right)\right], & r \geq 2R + \delta. \end{cases} \qquad (4b)$$

Here, ε is the dielectric constant of the continuous phase, κ is the Debye-Huckel inverse screening length, δ is the protein-protein distance of closest approach, and B_2 is calculated from Eq. (2) with $V(r) = V_A(r) + V_R(r)$. In agreement with previous investigations, Eqs. (4) accurately describe our B_2 measurements over a wide range of ionic strengths with $A = 5kT$, $\delta = 0.1$ nm, and $q = 10.5$ [7,8]. At ionic strengths of 0.15 and $0.2M$, $\kappa R = 2.16$ and 2.49, respectively ($\kappa^{-1} = 0.79$ and 0.68 nm). Thus, R_g of PEG 12 000 is nearly an order of magnitude larger than the electrostatic screening length.

To investigate the effect of added polymer on protein interactions, the normalized lysozyme second virial coefficient $B_2/B_2^{\rm HS}$ (where $B_2^{\rm HS} = 16\pi R^3/3$) was measured as a function of PEG concentration and molecular weight at a fixed ionic strength of $0.2M$ (Fig. 1). For each polymer molecular weight, B_2 is a strikingly nonmonotonic function of polymer concentration. The attractive minimum in B_2 at roughly $c_p \cong c_p^*$ becomes deeper and shifts to lower polymer concentration, as the PEG molecular weight increases. To the best of our knowledge, this is the first observation of such complex B_2 behavior in polymer-protein suspensions.

As seen in Fig. 2, increasing the ionic strength from 0.15 to $0.2M$ results in nearly a factor of 2 decrease in the polymer-free second virial coefficient as expected from the effective potential of Eq. (4). Nevertheless, the qualitative dependence of B_2 on polymer concentration is unaffected by the change in ionic strength suggesting the physical mechanism giving rise to the nonmonotonic behavior in Fig. 1 is insensitive to modest changes in κR.

Combining Eqs. (1), (2), and (4), the predictions of the AO model for $B_2(c_p)$ can be deduced with no free parameters. As shown in Fig. 1, the AO potential predicts a monotonic decrease of B_2 with c_p, and significantly overestimates the attractive depletion strength even at low polymer densities in a manner which becomes more severe with increasing polymer chain length. The failure of the AO model is perhaps not surprising given its treatment of the polymer solution as an ideal suspension of small macromolecules modeled as impenetrable hard spheres.

We have also analyzed our experimental results in terms of the analytic PRISM integral equation theory [14]

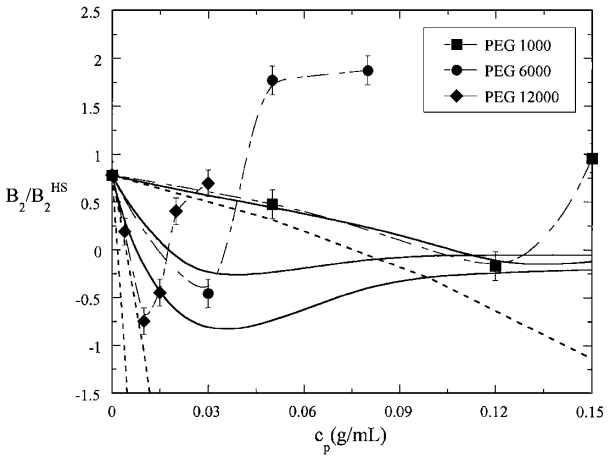

FIG. 1. Comparison of the predictions of the AO model (dashed lines) and thermal PRISM theory (solid lines) to the experimental data (symbols) for lysozyme in the presence of PEG at an ionic strength of $0.2M$ ($T = 25$ °C). The dot-dashed lines through the data points are drawn as a guide to the eye.

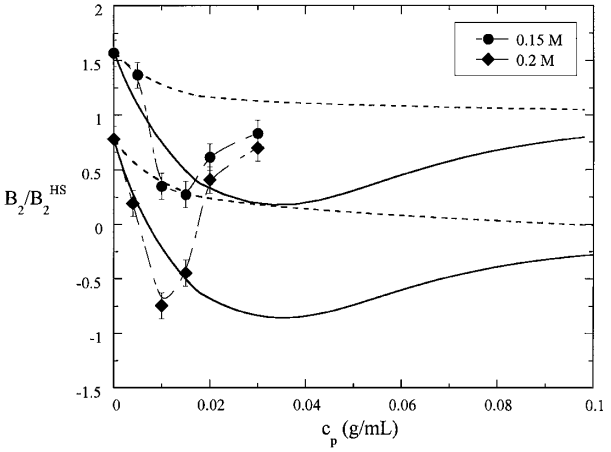

FIG. 2. Normalized second virial coefficient as a function of PEG 12 000 concentration at ionic strengths of 0.15 and 0.2M at 25 °C. Dashed (solid) curves are predictions of athermal (thermal) PRISM theory. The dot-dashed lines are a guide to the eye.

of depletion forces which employs a random walk model of polymer conformation, adopts pure excluded volume particle-particle and segment-particle interactions, and accounts for variable effective segment-segment interactions. Based on the polymeric version of the Percus-Yevick (PY) closure, the attractive depletion potential between hard particles is given by

$$U(r) = -kT \ln\left[1 + \frac{\pi z}{3}\left(\frac{R}{r}\right)\left(\frac{R}{\sigma}\right)e^{-(r-2R)/\xi_\rho^{\rm th}}\right]. \quad (5)$$

Far from any polymer-solvent demixing transition, the thermal mesh size, $\xi_\rho^{\rm th}$, reduces to its temperature-independent athermal analog, $\xi_\rho = \xi_\rho^{\rm ath}$, given below Eq. (3). Increases of $\xi_\rho^{\rm th}$ as a LCST phase boundary is approached are modeled [14] in a mean field manner as $\xi_\rho^{\rm th} = \xi_\rho^{\rm ath}(1 - T/T_s)^{-1/2}$, where $T_s(c_p)$ is the spinodal temperature for polymer-solvent phase separation. Theoretical expressions for $T_s(c_p)$ exist [10], but in this work we shall employ direct experimental estimates. Both the classic PY theory of hard spheres and the PRISM-PY theory of thread chains have been shown [15] to be equivalent to a simple Gaussian field theory of density fluctuations with the local excluded volume constraints rigorously enforced.

Substituting Eq. (5) into Eq. (2) yields the hard particle reduced second virial coefficient.

$$\frac{B_2}{B_2^{\rm HS}} = 1 - \frac{\pi z}{4}\left(\frac{\xi_\rho^{\rm th}}{\sigma}\right)\left[1 + \frac{\xi_\rho^{\rm th}}{2R}\right]. \quad (6)$$

B_2 depends sensitively on the ratio of thermal polymer mesh size to protein radius, $\xi_\rho^{\rm th}/R$, which itself is a function of polymer concentration, reduced temperature $T/T_s(c_p)$, and N. In the "protein limit" of $\xi_\rho^{\rm th} \gg R$, the second attractive term in Eq. (6) is dominant. If R_g/R is sufficiently large, the theory predicts B_2 is a nonmonotonic function of polymer concentration, even in the athermal limit [14]. This arises from a competition between the strength of the depletion attractions which increase monotonically with polymer density, and their spatial range which decreases for $c_p > c_p^*$ due to physical mesh formation. For athermal solutions Eq. (6) predicts the minimum in B_2 occurs near the onset of this competition at $c_p \sim c_p^*$ and monotonically deepens and shifts to lower polymer concentrations as N is increased. If the polymer solution is sufficiently "close" to a demixing boundary, then the minimum feature in B_2 weakly shifts to close to the critical polymer concentration c_{pc} and is significantly enhanced in depth. Physically this follows since the thermal enhancement of the polymer density fluctuation correlation length is maximal at c_{pc} and decreases sharply above and below the critical composition. In application of the theory to our experiments, the smallness of the protein ($R < R_g$) and the closeness of the system to a spinodal line both play a role in determining the observed behavior of the B_2 attractive minimum feature, although the latter effect is much more important.

To evaluate the significance of thermal fluctuations on depletion forces, the LCST binodal (cloud point) curves for PEG 6000 and 12 000 were determined by visual inspection of polymer/buffer solutions at an ionic strength of 0.2M. Results for the PEG 12 000 sample are shown in Fig. 3, where the binodal curve is in good agreement with prior work [16]. With decreasing polymer molecular weight, the LCST phase boundary shifts to higher temperature, and the minimum of the binodal curve shifts to higher polymer concentration [16].

The spinodal curve for PEG 12 000 was also obtained by measuring the static structure factor in the limit of zero angle, $S(0)$, in the absence of protein. The mean field spinodal temperature, $T_s(c_p)$, was estimated by linear extrapolation to zero of the $1/S(0)$ (in arbitrary units) versus the $1/T$ plot. The critical temperature is found not

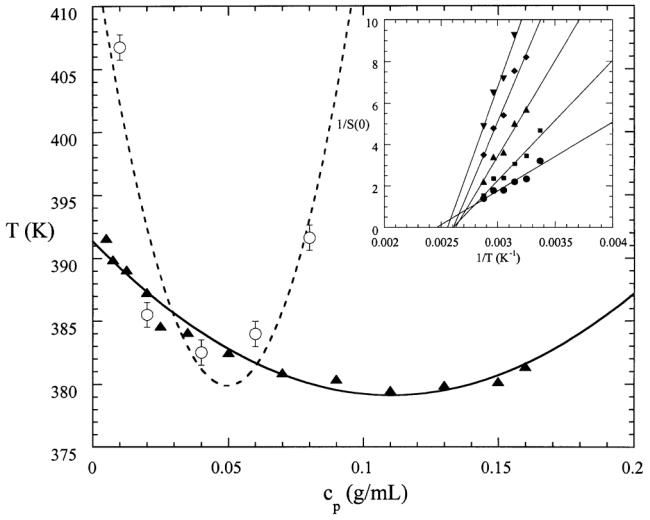

FIG. 3. Phase diagram for PEG 12 000. Solid line and filled symbols mark the cloud point temperatures as a function of polymer concentration; dashed curve and open symbols mark the spinodal curve obtained by extrapolation as shown in the inset.

to be the lowest temperature on the binodal curve. Such a complex phase diagram is not uncommon in ternary and higher mixtures such as our salt-water-polymer solution; similar behavior has been found in polydisperse polymer blends [17]. From Fig. 3, we estimate that $T_c = 379$ K and the critical polymer concentration $c_{pc} \cong 0.04\ \mathrm{g\,cm^{-3}}$, close to c_p^*. Thus, the ratio $T/T_s = 0.78$ at 25 °C, yielding a thermal mesh size at c_{pc} of $\xi_\rho^{\mathrm{th}} = 2.1\xi_\rho^{\mathrm{ath}} \cong 7$ nm $\cong 4R$. As the polymer concentration increases or decreases from its critical value the thermal mesh length rapidly decreases towards its athermal value.

Combining Eqs. (2) and (4)–(6) with $V(r) = U(r) + V_A(r) + V_R(r)$ and all the characterization data, the predictions of thermal PRISM theory can be evaluated for PEG 12 000 with *no adjustable parameters.* In the athermal limit (Fig. 2), no minimum in B_2 appears, because R_g/R does not exceed the required threshold [14]. Predictions of thermal PRISM theory are compared with the experimental data in Figs. 1 and 2. The experimentally obtained T_s was fit to a quadratic form $T_s(c_p) = T_c + b(c_p - c_{pc})^2$ with $T_c = 379$ K, $b = 1.5 \times 10^4\ \mathrm{K\,(g\,mol^{-1})^{-2}}$, and $c_{pc} = 0.04\ \mathrm{g\,cm^{-3}}$. Spinodal curves for PEG 1000 and 6000 solutions were indirectly estimated with a similar quadratic form of T_s by setting $c_{pc} = c_p^*$, and $T_c = 422$ K and 388 K for PEG 1000 and 6000, respectively. The former values of T_c are in agreement with prior measurements [16]. As seen in Fig. 1, thermal PRISM theory is successful in describing the depth and qualitative location of the minimum and its dependence on polymer molecular weight and ionic strength (Fig. 2). This suggests the strong N-dependence of B_2, and its nonmonotonic variation with c_p, as primarily due to thermal polymer concentration fluctuations. This idea is further supported by our measurements [8] of the temperature dependence of B_2 at a c_p near the minimum for PEG 6000 and 12 000. A monotonic deepening of the minimum in B_2 is observed as the solution is heated towards the phase boundary from 288 to 308 K, in nearly quantitative accord with the theoretical predictions [8]. However, the theory, and/or simple polymer-protein model employed, fails to account for the steep repulsive upturn of B_2 at higher concentrations.

In summary, we have characterized for the first time a thermodynamically relevant strength of depletion interactions between a small globular protein and relatively large water soluble polymers as a function of temperature, polymer concentration, molecular weight, and solution ionic strength. The central novel experimental result is the observation that the protein second virial coefficient passes through a sharp minimum with increasing polymer concentration. This minimum deepens with polymer chain length and heating, and occurs close to the N-dependent semidilute crossover or critical polymer concentration. The classic AO depletion model fails to capture these observations, but predictions of polymer integral equation theory are in good qualitative, and reasonable quantitative, agreement with the data. This agreement suggests that the strength of polymer-mediated attractive forces between small proteins can be tuned by rational manipulation of the mesh size of polymer solutions by modest pretransitional thermal polymer concentration fluctuations even 75–100 °C away from the critical temperature. This effect may be exploited in a variety of scientific and technological contexts, including the important problem of optimizing protein crystallization conditions.

A. M. K. and C. F. Z. were supported by NASA Grant No. NAG 8-1376. A. P. C. and K. S. S. acknowledge support from the U.S. DOE via the University of Illinois at Urbana-Champaign Materials Research Laboratory Grant No. DEFG02-96ER45439.

*Present address: Department of Chemistry, SUNY College of Environmental Science and Forestry, 1 Forestry Drive, Syracuse, NY 13210.

[1] A. P. Gast, C. K. Hall, and W. B. Russel, J. Colloid Interface Sci. **96**, 251 (1983); C. Cowell, F. K. R. Li-In-On, and B. J. Vincent, J. Chem. Soc. Faraday Trans. 1 **74**, 337 (1978); W. C. K. Poon, A. D. Pirie, and P. N. Pusey, Faraday Discuss. **101**, 65 (1995); A. L. Ogden and J. A. Lewis, Langmuir **12**, 3413 (1996).
[2] S. Asakura and F. Oosawa, J. Polym. Sci. **33**, 183 (1958).
[3] J. F. Joanny, L. Leibler, and P. G. de Gennes, J. Polym. Sci. Polym. Phys. Ed. **17**, 1073 (1979); G. J. Fleer, J. H. M. H. Scheutjens, and B. Vincent, ACS Symp. Ser. **240**, 245 (1984).
[4] A. Milling and S. Biggs, J. Colloid Interface Sci. **170**, 604 (1995).
[5] R. Verma, J. C. Crocker, T. C. Lubensky, and A. G. Yodh, Phys. Rev. Lett. **81**, 4004 (1998).
[6] A. Polson, G. M. Potgieter, J. F. Largier, G. E. F. Mears, and F. J. Joubert, Biochim. Biophys. Acta **82**, 463 (1964); A. McPherson, Methods Enzymol. **114**, 112 (1985).
[7] D. F. Rosenbaum and C. F. Zukoski, J. Cryst. Growth **169**, 752 (1996).
[8] A. M. Kulkarni, A. P. Chatterjee, K. S. Schweizer, and C. F. Zukoski (to be published).
[9] K. S. Schweizer and J. G. Curro, Adv. Chem. Phys. **98**, 1 (1997).
[10] A. P. Chatterjee and K. S. Schweizer, Macromolecules **31**, 2353 (1998).
[11] P. G. deGennes, *Scaling Concepts in Polymer Physics* (Cornell University, New York, 1979).
[12] B. Vincent, P. F. Luckham, and F. A. Waite, J. Colloid Interface Sci. **73**, 508 (1980).
[13] M. L. Grant and D. A. Saville, J. Colloid Interface Sci. **171**, 35 (1995); C. M. Roth, J. E. Sader, and A. M. Lenhoff, J. Colloid Interface Sci. **203**, 218 (1998); R. B. McClurg and C. F. Zukoski, J. Colloid Interface Sci. **208**, 529 (1998).
[14] A. P. Chatterjee and K. S. Schweizer, J. Chem. Phys. **109**, 10 464 (1998); **109**, 10 477 (1998); Macromolecules **32**, 923 (1999).
[15] D. Chandler, Phys. Rev. E **48**, 2898 (1993).
[16] S. Saeki, N. Kuwahara, M. Nakata, and M. Kaneko, Polymer **17**, 685 (1976).
[17] D. Schwan, K. Mortensen, T. Springer, Y. Madeira, and R. Thomas, J. Chem. Phys. **87**, 6078 (1987).